Hindawi
Advances in Meteorology
Volume 2023, Article ID 5372701, 17 pages
https://doi.org/10.1155/2023/5372701

Research Article

Spatial and Temporal Analysis of Rainfall Variability and Trends for Improved Climate Risk Management in Kayonza District, Eastern Rwanda

Joseph Ndakize Sebaziga,[1,2] **Anthony Twahirwa**,[1,3] **Jonah Kazora**,[1,4] **Frank Rusanganwa**,[1,4] **Mathieu Mugunga Mbati**,[1] **Steven Higiro**,[1] **Sandrine Guhirwa**,[1] **Jean Claude Nyandwi**,[1] **and Jean Marry Vienney Niyitegeka**[1]

[1]*Weather, Climate Service and Application Division, Rwanda Meteorology Agency, P.O. Box 898, Kigali, Rwanda*
[2]*School of Science and Technology, University of Rwanda, P.O. Box 3900, Kigali, Rwanda*
[3]*University of Nairobi, P.O. Box 30197, Nairobi 00100, Kenya*
[4]*Collaborative Key Laboratory of Meteorological Disaster, Ministry of Education (KLME), Joint International Research Laboratory of Climate and Environmental of Meteorological Disasters (CIC-FEMD), University of Information Science and Technology, Nanjing 210044, China*

Correspondence should be addressed to Joseph Ndakize Sebaziga; ndakize88@gmail.com

Received 10 May 2023; Revised 24 August 2023; Accepted 4 September 2023; Published 19 September 2023

Academic Editor: Marzuki Marzuki

The variability, intensity, and distribution of rainfall have drawn a lot of interest globally and especially in nations where rainfed agriculture is the norm. This article uses rainfall data from the Rwanda Meteorology Agency for the years 1981 to 2021 to delineate and analyze rainfall variability and trends in the Kayonza District. The time series were grouped using the *K*-means clustering technique based on computed Euclidean distance, the total within-cluster sum of squares, and the elbow plot technique to determine the optimal number of clusters. The coefficient of variation measures was employed to analyze rainfall variability, while Sen's slope and the Mann–Kendall (MK) test were used, respectively, to find trends and changes in magnitude. The results indicated four near homogeneous zones named region one to four. The dry seasons indicated higher variability compared to rainy seasons and annual rainfall total with a variability of 128–142% over the southeastern part during June to August (JJA) season, while a variability of 16–48% was observed over most of the district during both annual and rainy seasons. It was further noted that the areas in the central part of the Kayonza District indicated a significant increasing trend at a significance level of 95% and above during January to February (JF), September to December (SOND), and on annual basis, while March to May (MAM) and JJA season exhibited no significant trend. The findings of this study are essential for creating adequate mitigation strategies to lessen climate change's effects on agriculture as well as other socioeconomic sectors.

1. Introduction

The sub-Saharan Africa (SSA) countries have seen the effects of climate change, with numerous extreme events causing declines in crop production quality and quantities, with much bigger implications on the lives of smallholder farmers [1]. In SSA, the rainfed agricultural sector is the utmost principal source of livelihood for the human population [2–4]. The spatial and temporal variability of the rainfall distribution in East Africa countries (EA) is more pronounced, and catastrophic events, such as destructive droughts and floods, occur more frequently leading to detrimental effects on socioeconomic sectors as well as human and animal deaths [5–9]. The dynamics and evolution of the climate system, as well as the variability and predictability that go along with it, can all be better understood with an improved understanding of rainfall variability and trend [10, 11]. Sea surface temperatures (SSTs) are frequently used predictors of seasonal rainfall over the EA region and other parts of the tropics [12, 13] with enhanced and depressed seasonal rainfall over EA region been linked with the warming and cooling over the western Indian Ocean and Eastern Atlantic Oceans [14] in addition to winter or northeast (NE) monsoon during December to February and summer or southeast (SE) monsoon during June to August [15]. Over EA region, El Niño and positive Indian Ocean Dipole (IOD) are linked to enhanced seasonal rainfall, while La Nina and negative IOD are associated with reduced seasonal rainfall over the region and other neighboring areas [7, 14, 16–19]. Despite the fact that the effects of tropical cyclones on the region's weather vary depending on the time of year, where they are located, and the associated large-scale flow, cyclones that move into the Mozambique channel have an impact on the region's weather from March to May by causing low level diffuse flow, while rainfall tends to increase during the months of December and January, leading to frequently observed flooding in the area [13]. On the internal climate forcing mechanisms, volcanoes, for example, have been found to affect climate and have the potential to affect the skill of certain seasonal forecasts made after large eruptions [20]. The intraseasonal rainfall variability over the region are associated with equatorial Rossby waves which exhibit a dominant 10–30-day time scale periodicity [8, 21], while a higher association between Madden–Julian oscillation (MJO) with rainfall was observed over the west of the region [22].

The rainfall in Rwanda has a northwest-east slant with more rainfall in the northwestern than the eastern side of the country [18]. Its distribution is controlled by global to local processes such as position and intensity of anticyclones such as St. Helena, Mascarenes, Azores and Siberian [23–25], intertropical convergence zone [26], and Lake Victoria and Congo Air mass [23, 24]. Rwanda experiences two major rainy seasons in a year, March to May (long rainy season) and September to December (short rainy season), and two dry seasons, June to August (long dry season) and January to February (short dry season) [18, 19, 27– 29], with April and November being the monthly rainfall peak for March to May and September to December rainy seasons, respectively [30, 31]. Rainfall seasons in Rwanda alternate due to the movement of the intertropical convergence zone (ITCZ) crossing the equator from North to South and vice-versa [26], and its passage results in two rainy seasons (MAM and SOND) [31, 32]. MAM rainy season occurs when ITCZ passes from south to north hemisphere, while the SOND rainy season occurs when passes from north to south hemisphere [12]. During the dry season, the climate of Rwanda is dry mainly in Eastern lowlands and is influenced by dry anticyclones of Saint Helena and Azores, while the western highlands receive some rainfall resulting from Saint Helena anticyclones passing over lake Kivu from Atlantic Ocean [18]. Rainfall characteristics over Rwanda have been the subject of several recent studies [8, 19, 27, 28, 31, 33, 34]. Since the economy of the Kayonza District is heavily dependent on the agriculture industry, rainfall fluctuation will have a variety of consequences on farming activities and other sectors that support the district's economy. None of the previous studies have concentrated on understanding rainfall characteristics over the Kayonza District which is one of the dry areas in the eastern region of the country. Furthermore, previous research has indicated that rainfall and temperature vary geographically across the country due to the complex topography [31] with the eastern region receiving a low amount of rainfall and high temperature [25, 31] and that the mean rainfall significantly reduces when topography reduces [31]. This would also motivate this present study to characterize this region by focusing on the interannual variation and trend of rainfall and including dry seasons which serves as the postharvest period of the previous rainy season. In addition, none of the previous work has attempted to delineate this region into near homogeneous zones which would be of great impact for decision-making and agricultural management and practices.

2. Materials and Methods

2.1. Study Area. The research was carried out in the Kayonza District (1°51′S, 30°39′E), in the Eastern Province of Rwanda, with an altitude ranging between 1400 and 1600 m [35]. The Kayonza District (Figure 1), being one of the seven districts that make up the Eastern Province of Rwanda, has an average area of 1,937 km^2 and a total population of 344,157 people, with 34,008 of them living in urban areas and 310,149 in rural areas, at a density of 178 people per km^2 [36]. With the exception of the East, where some slopes are stiff and stony, the relief is characterized by plates at broad summits and hills with smooth slopes. The district is the home for numerous small interior lakes such as Cyabatanzi, Hago, Ihema, Kibare, Kivumba, Rwibishuhe, Shakani, and Kabigabiro, whereas to the west, the lake Muhazi separates Kayonza from the neighboring districts. The rainfall over Kayonza shows a bimodal characteristic similar to other regions of the country, with April and November being the peak months for each of the two wet seasons extending from March to May (MAM) and September to December (SOND), respectively, while January and February (JF) and June to August (JJA) are the dry seasons (Figure 2) confirming other previous findings [18, 19, 27–29, 31]. Rainfall over Kayonza exhibits an increasing trend while it is inversely correlated to the normalized differential vegetation index [37] with a lower frequency in rainy days [29] and is projected to increase by 29% through the 21st century [38]. The majority of the population relies on agriculture, small-scale traders, and subsistence pastoralists for a living, with maize being cultivated primarily through effective land consolidation [39]. While forest savannah makes up the majority of the vegetation, half of Akagera National Park is a hub of different species of flora and wildlife [36]. In general, increase in rainfall [40] and decrease in mean temperatures [41] were seen particularly in highland, western, and regions near Lake Kivu, causing more flooding. In contrast, decreased rainfall, aridity index, and warming characteristics were seen in the eastern low land region, where the Kayonza District is located which leads to crop failure and decreased yield production [40, 41]. In terms of climatic zones, previous work has delineated Rwandan climate into four [25] and five [42] near homogeneous zones with the entire eastern region extending to Kigali city falling in the East-Rwandan dry and hot lowland zone [25, 42]. The variations in precipitation intensity and frequency, along with the agricultural reforms implemented in Rwanda, may have an impact on the trends in yields of the country's key food crops at the time [43]. The majority of crop yields in the eastern lowland are predicted to decrease during the SOND season due to expected declines in mean rainfall and the number of rainy days, while bean, maize, and Irish potato yields are predicted to increase during MAM due to anticipated increases in the mean rainfall and the number of rainy days [44].

2.2. Data. The daily gridded rainfall dataset which was accumulated to monthly, seasonal, and annual total were obtained from Rwanda Meteorology Agency (Meteo Rwanda) with a spatial resolution of 0.0375 degrees (~4 km) for the period of 1981 and 2021. This dataset was generated by merging quality-controlled observed data with satellite rainfall estimates data from Tropical Applications of Meteorology using SATellite (TAMSAT). The used rainfall dataset was used in the previous studies [27, 34, 45–48]. More information on the generation of the dataset is found in [27].

2.3. Methods. Several studies have used the *K*-means clustering method to delineate climate variable into near homogeneous zones by combining comparable data points to identify the underlying pattern [49–54]. To implement the *K*-means clustering technique, the following steps are required. First, we find the center of the first cluster and repeat the process. Depending on the average value of the objects in the cluster, we assign each object to the cluster to which it is most comparable. We restructure the cluster means and then calculate the items' average value for each cluster. We repeat the process until no further change is observed [52–54]. *K*-means clustering is utilized in this case to group the time series according to the Euclidean distance and the total within-cluster sum of squares (TWCSS) [52, 54]. The closest cluster is assigned to each data point while reducing intracluster variation. More information of the use of *K*-means clustering can be found in [51, 55, 56]. In the present study, daily rainfall and temperature data were used to generate monthly data which in turn were aggregated to the seasonal and annual time scale. To delineate the study area into near homogeneous zones, rainfall, maximum temperature, and minimum temperature data were considered. To avoid giving more weight towards the largest values, input data were standardized. The seasonal and annual rainfall climatology for each grid was generated by aggregating monthly rainfall to seasonal rainfall for each grid. To understand the variability in rainfall, the coefficient of variation measure (CV) which measures the degree of variability in a dataset was employed in the present study. The simple linear regression method was applied to present the graphical trend for seasonal and annual rainfall generated for each grid representing a corresponding near homogeneous zone (region). The advantage of this method is that it provides quick visual observations of the presence of a trend in each time series. Mann–Kendall (M.K), a nonparametric rank-based test, was employed under this study to test the statistical significance of the observed trends where positive values show an upward slope, while a negative value indicates a downward slope [57–60]. This method has been widely used in previous research over Rwanda [29, 45, 46, 61].

3. Results and Discussion

Our goal in this research was to determine the ideal number of zones, and we employed the *K*-means clustering technique with various cluster counts (k) and calculated the total within the sum of squares for each k value and plotted the optimum number of clusters using the elbow plot technique. The results obtained by the process of clustering rainfall over the Kayonza District are presented in Figures 3–5, respectively. The distance between points and the centroid in the same cluster and in different clusters is represented in two dimensions using the centroid of clusters as presented in (Figure 3) where four clusters representing rainfall and temperature characteristics in the Kayonza District are indicated with the first two components explaining 81.34% of the variability.

Finally, the optimal number of clusters is thought to be the k value at the bend (elbow joint) in the figure. The total sum of squares distance in elbow plot falls as the value of k grows (Figure 4), although there is a bend at $k = 4$. It demonstrates how adding more clusters will result in a modest reduction in the sum of squares. Consequently, four can be thought of as the ideal number of clusters.

The obtained four optimum numbers of clusters corresponding to four near homogeneous zone in the Kayonza District are represented on the spatial map of the study area using ArcGIS software (Figure 5).

Table 1 presents the seasonal rainfall characteristics over the Kayonza District for different near homogeneous zones. During the JF season, rainfall ranges from 32 mm (R4) to 396 mm (R3) with a mean range of 129 mm (R4) to 149 mm (R3) and a standard deviation of 61 mm (R2) to 75 mm (R3). Rainfall varies from 46% (R1 and R2) to 50% (R3) and contributes 15% (R1 and R4) to 16% (R2 and R3). During MAM, rainfall ranges from 101 mm (R2) to 598 mm (R1) with a mean range of 329 mm (R2) to 365 mm (R3) and a standard deviation of 81 mm (R4) to 97 mm (R1). Rainfall varies from 24% (R4) to 28% (R2) and contributes 38% (R4) to 41% (R1 and R2). During the JJA season, rainfall ranges from 0 mm (R3) to 8 mm (R1) with a mean range of 50 mm (R4) to 64 mm (R3) and a standard deviation of 45 mm (R4) to 58 mm (R3). Rainfall varies from 83% (R2) to 98% (R1) and contributes 6% (R1 and R4) to 7% (R2 and R3). During SOND, rainfall ranges from 73 mm (R2) to 580 mm (R1) with a mean range of 286 mm (R2) to 366 mm (R4) and a standard deviation of 79 mm (R4) to 110 mm (R1) with

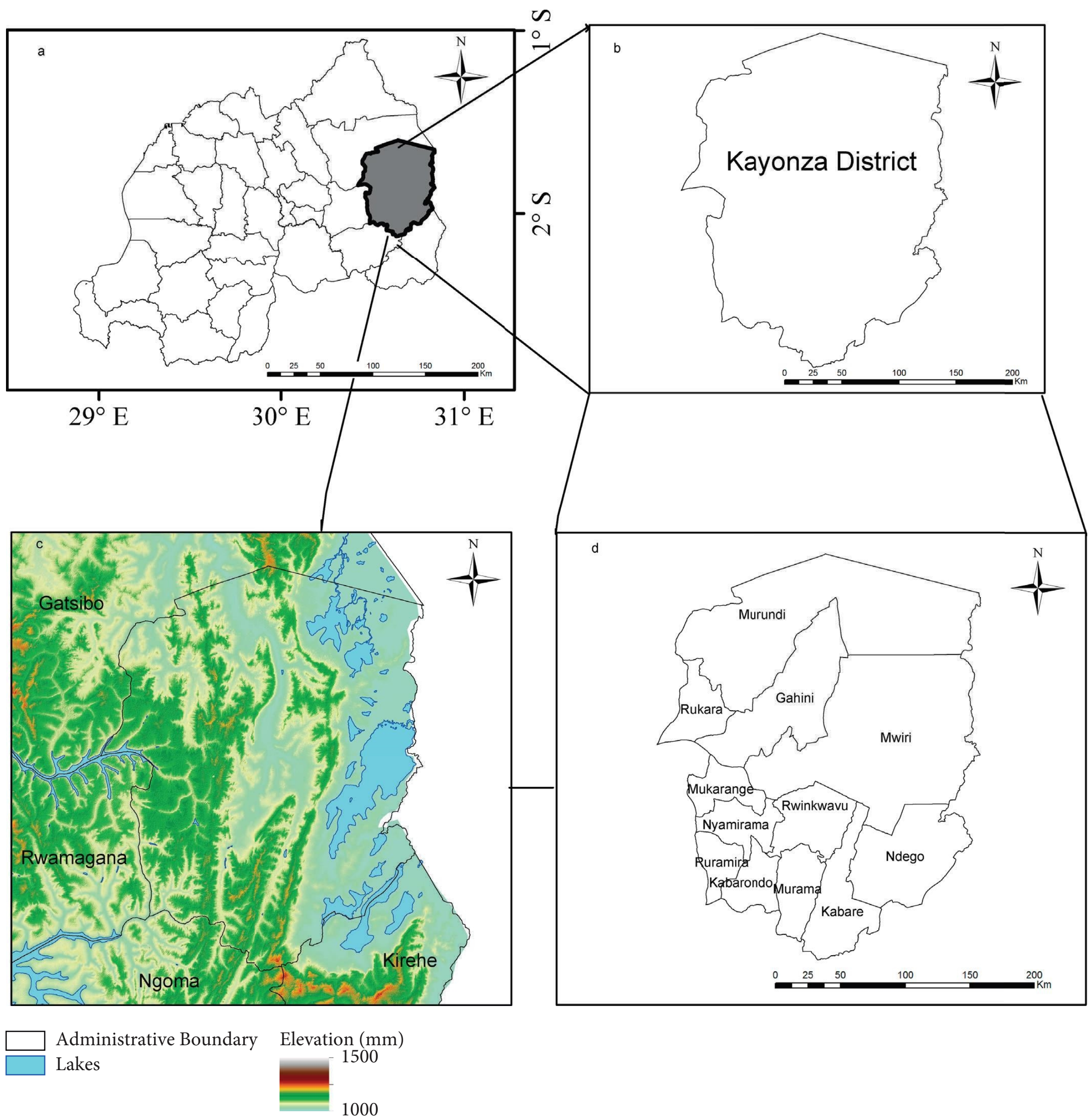

FIGURE 1: Map of Rwanda presenting the geographical local of the Kayonza District (a), limitation of the Kayonza District (b), hydrographical and topographic features of Kayonza and neighboring districts (c), and the administrative boundary of sectors in the Kayonza District (d).

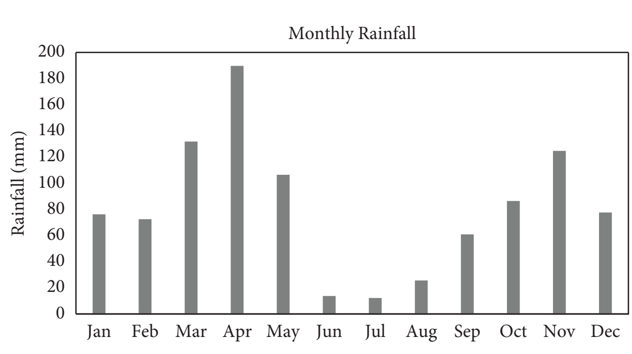

FIGURE 2: Monthly rainfall climatology over the Kayonza District from 1981 to 2021.

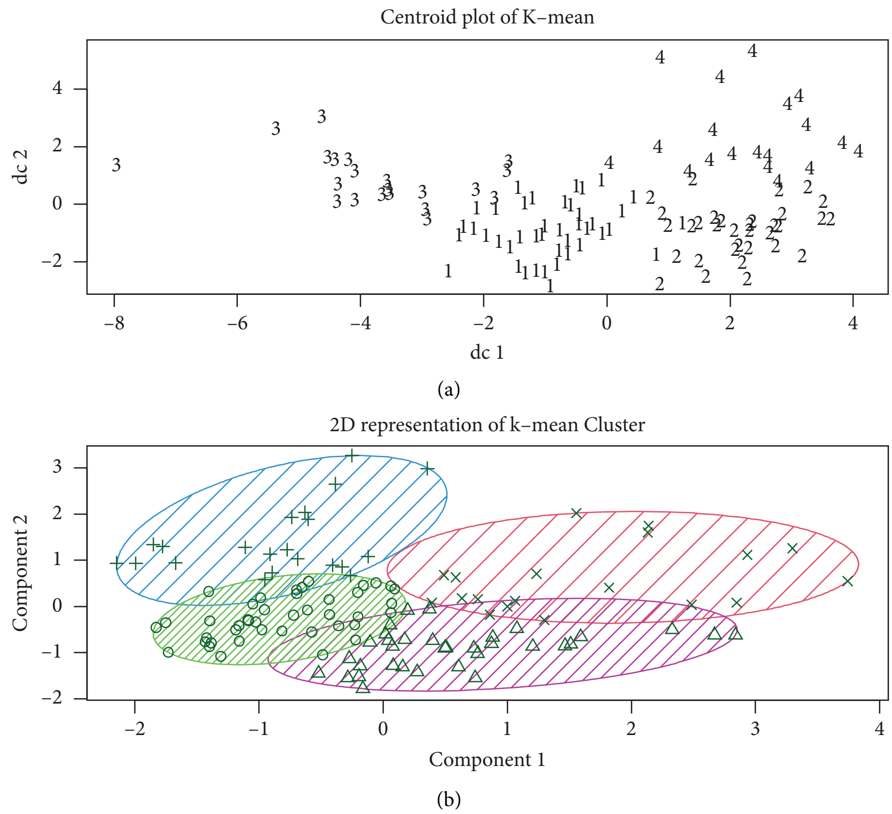

FIGURE 3: Two dimensions representation of the cluster. The number in (a) represents the assignment of each point in a cluster, and the points in each cycle represent the grid point clustered in the same cluster over the Kayonza District. (a) Centroid plot of *K*-means. (b) 2D representation of the *k*-means cluster.

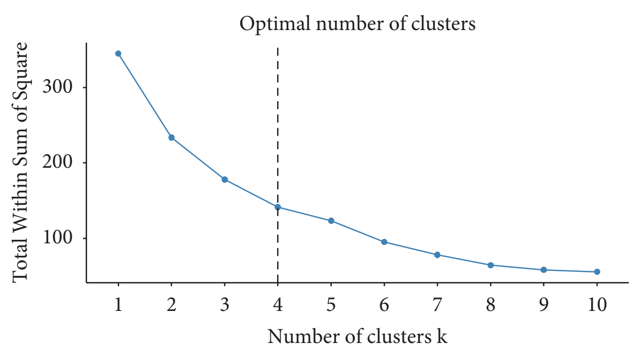

FIGURE 4: Example for elbow plot to check the optimal number of clusters (k). The dotted line indicates the elbow joint, and it will help find the *k* value over the Kayonza District.

a varies from 22% (R4) to 33% (R2 and R3) and contribute 36% (R3 and R3) to 41% (R4).

The spatial distribution in seasonal and annual mean rainfall is presented in Figure 6. Both short dry seasons spanning the month of January to February (JF) and long dry season extending from the month of June to August indicated a lower mean rainfall amount ranging between 20 and 100 mm over the northwester part of the district (R4) increasing towards the rest of the country (R1 to R3) with a maximum mean seasonal rainfall of 180 mm. These two dry seasons are mainly helpful for the agricultural purpose as they serve as the postharvest period for both the SOND and MAM seasons, respectively. During the long rain season (MAM), the southwestern part of the district (R1) revealed higher mean seasonal rainfall (500–580 mm) decreasing to the rest of the R1 and eastern part of the district (R3), while the southern part of the district in R2 and R3 extending toward the central part in R2 and northern areas in R4 exhibited lower seasonal mean rainfall (260–340 mm). The short rain season (SOND) indicated lower seasonal mean rainfall over the southern part of the district in R2 and R3 extending towards the central part in R2 and northern areas in R4 with a mean range of 180–340 mm, while the eastern part of the country

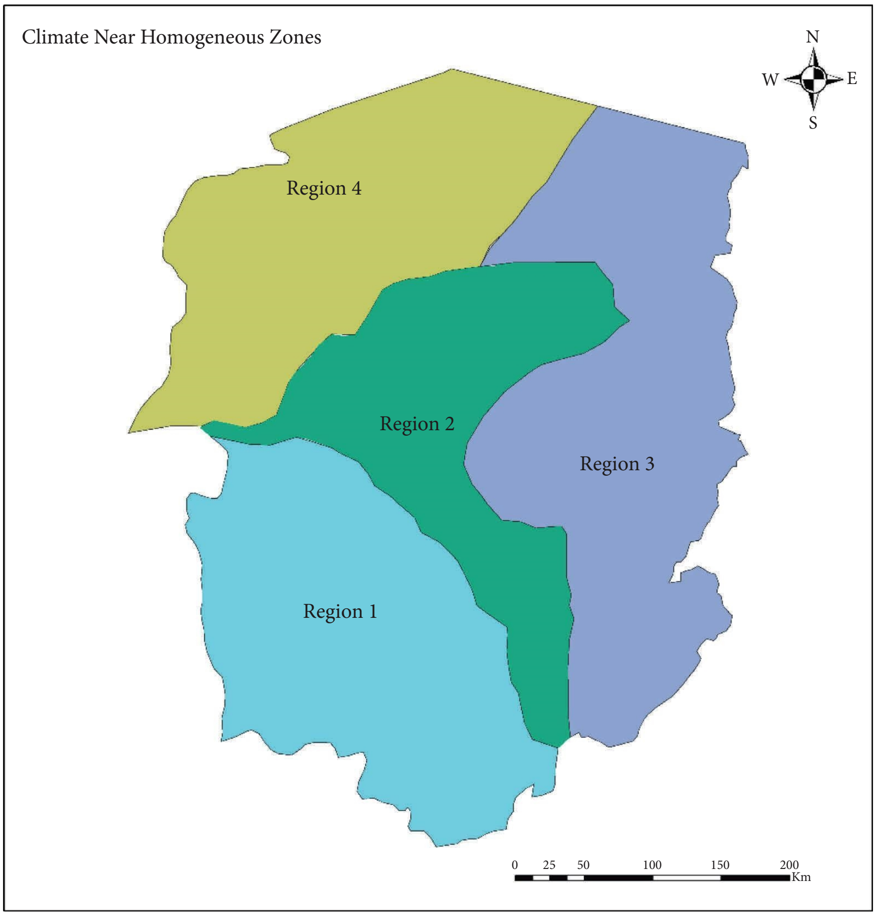

Figure 5: Climatic classification of the Kayonza District based on the data from 1981 to 2021. Four near homogeneous zone in the Kayonza District, clear green color to the west (region 1, R1), dark green color (region 2, R2), red color to the east (region 3, R3), and blue color to north (region, R4).

(R3) and part of the northwestern (R4) and northern areas of R1 show moderate rainfall (340–420 mm) increasing to the southwestern side of the district (R1) with a mean rainfall of 500–580 mm. The two rainy seasons show that the southern through the central part extending to the northern areas receives quite low rainfall which would be challenging regions for farming activities. On annual basis, the northwestern region (R4) indicated reduced rainfall (620–720 mm) increasing towards the central and southern part of the district (R2) with a mean annual rainfall of 720–820 mm. Moderate rainfall (820–1120 mm) was observed over the rest of all regions except for the western part of the R1 which indicated rainfall reaching 1200 mm. The mean rainfall over the area is in the range of the previous finding with certain locale areas diverging markedly from the annual averages [25, 42]. Based on the ranges in the observed rainfall amount, agriculture can be practiced. The adequate water supply and temperatures favor the cultivation of moisture-loving crops [42]. Similar to the results obtained by [27, 31], the western side of the district registers higher rainfall compared to other regions which show that topography remains one of the rainfall controlling factors of the area.

In terms of rainfall variability as presented in Figure 7, the JF short dry season exhibits moderate variability over the northwestern part of the district (R4) with a magnitude of 64–80% reducing towards the eastern part (R3) and the rest of the R4 at a variation rate of 48–64%, while the northern part of R3 and most of the R1 show lower variation (32–48%). The long dry season shows more variability compared to the rest of seasons with a magnitude of 128–144% over the southeastern side of the district (R3) reducing towards the central and western sides of the district (R1–R3) with a variation magnitude of 96–128%, while lower variability was observed over the northern section of the district (80–96%). During MAM season, except for a small portion of the northwestern (R4) which indicated a variation of 32–48%, the rest of the regions experienced quitelower variability ranging between 16 and 32%. Similarly, SOND season indicated more variability over the southern part of the district (R2 and R3) and over the northwestern areas (R4) with a variation magnitude of 32–48%, while the rest of the region indicated lower variation with a magnitude of 16–32%. On the annual scale, the whole district shows a throughout less variation in rainfall with a magnitude of 16–32%. The rainfall variability

Table 1: Seasonal and annual rainfall characteristics with maximum (MAX), minimum (MIN), long term mean (LTM), standard deviation (SD, in mm), coefficient of variation (CV in %), seasonal contribution to annual mean rainfall (Cont. in%), trend magnitude (Q in mm/year) and significance (Sig, at 99% (**), 95% (*) and greater than 90% (+) confidence level respectively) for the four near homogeneous climatic zone (R1–R4) from 1981–2021 over Kayonza district.

Season	Region	Seasonal rainfall characteristics MAX (mm)	MIN (mm)	LTM (mm)	SD (mm)	CV (%)	Cont. (%)	Q (mm/year)	Sig
JF	R1	318	39	135	62	46	15	−0.3	
	R2	271	34	131	61	46	16	0.5	
	R3	396	52	149	75	50	16	2.6	**
	R4	288	32	129	62	48	15	1.4	
MAM	R1	598	149	360	97	27	41	−0.5	
	R2	541	101	329	91	28	41	−1.8	
	R3	557	109	365	96	26	40	−0.7	
	R4	490	190	335	81	24	38	−0.5	
JJA	R1	225	8	52	51	98	6	−0.1	
	R2	227	2	56	47	83	7	0.3	
	R3	258	0	64	58	89	7	0.8	
	R4	210	6	50	45	90	6	0.5	
SOND	R1	580	123	332	99	30	37	−0.7	
	R2	561	73	286	96	33	36	1.9	
	R3	549	121	331	110	33	36	3.5	+
	R4	532	235	366	79	22	41	0.2	
ANNUAL	R1	1412	381	887	203	23	—	−1.2	
	R2	1235	216	800	200	25	—	2.2	
	R3	1482	312	913	237	26	—	7.6	*
	R4	1175	571	883	144	16	—	3. 1	

magnitude observed over the Kayonza District differs from the findings of the previous study which reported no conclusive evidence on rainfall variability in the Eastern province [29]. The more fluctuations in rainfall over the Eastern were thought of being probably linked to sunspots [25]. This higher variability during dry seasons may greatly affect the postharvest activities for agricultural production realized during the wet seasons and would explain the inconsistence in the temporal distribution of rainfall during the subsequent rainy season. More energy is required during the postharvest period to transport and, ultimately, dispose of the harvested food, which can result in the loss of resources used to produce food that will not be eaten and badly impact farmers' livelihoods and significantly worsen food insecurity. Farmers can be taught how to reduce food loss and use climate-smart agricultural practices in order to increase sustainable productivity and lower greenhouse gas emissions from the agricultural sector. Any solution that truly addresses postharvest loss should take into account the relationship between food security and climate change in order to inform investment opportunities and practical strategies that can effectively reduce postharvest losses. Similar observations linking postharvest loss to climate variability and change have been made by [62–66].

The spatial distribution in seasonal and annual rainfall trend is presented in Figure 8. During the JF season, the central part of the Kayonza District indicated a significant increasing trend with a magnitude of 2-3 mm/year, while the norther part of the district indicated 0-1 mm/year and 1-2 mm/year over the southern part of the district, respectively. This observed increase in the rainfall would explain the current observed increased rainfall during the short dry season of JF which would extend the SOND seasons and would affect the postharvest period of the growing season commonly known as season B for agricultural purpose and would also affect the starting period of the MAM season commonly known as season A for agricultural purposes. During the long rain season (MAM), the northern region registered a decreasing trend ranging from 4 to 2 mm/year with few pockets of this areas being significant, while the central part extending to southern and southeastern regions observed a nonsignificant increase with a magnitude of 0–2 mm/year. The long dry season spanning through JJA indicated an increasing trend of 1-2 mm/year over the central parts of district (R1, R2, and R3), while the rest of the district indicated a reduced rainfall with a magnitude of -1-0 mm/year. The short rainy season extending throughout the SOND showed a general increase in rainfall with a significantly positive trend over the central part of the district with a Sen's slop magnitude of 3–6 mm/year. On the annual time scale, the southern part of the northern region showed a nonsignificant decrease of 4–0 mm/year, while the extreme north registered a positive trend of 0–6 mm/year, a significant upward trend over the central part experiencing an upward trend of 10–16 mm/year, while the southern region extending to the central part increased with a magnitude of 6–10 mm/year at a significance level of 95% and above. The observed decreasing trend during MAM and increasing during the SOND season confirms the previous findings [19].

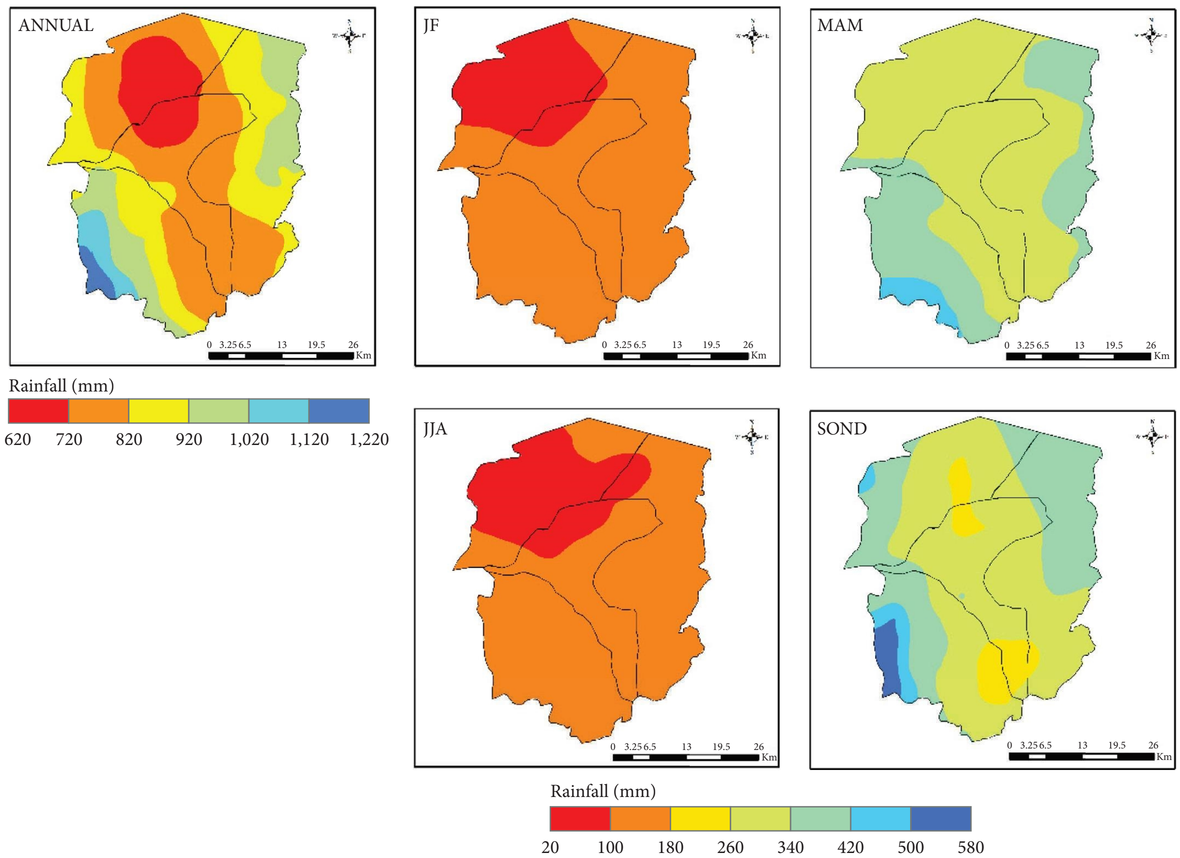

FIGURE 6: Spatial mean rainfall distribution during January to February (JF), March to May (MAM), June to August (JJA), September to December (SOND), and annual rainfall over the Kayonza District from 1981–2021. JF, MAM, JJA, and SOND share the same legend.

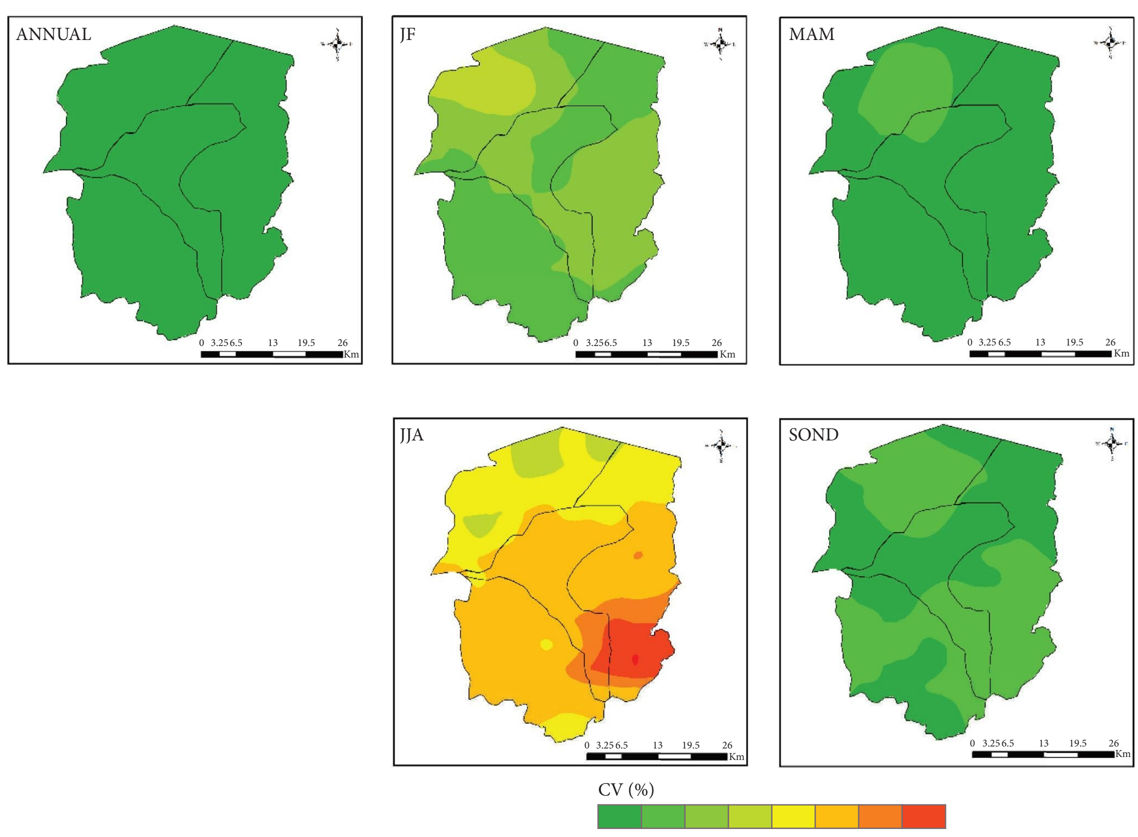

FIGURE 7: Spatial rainfall variability during January to February (JF), March to May (MAM), June to August (JJA), September to December (SOND), and annual time scale over the Kayonza District from 1981 to 2021.

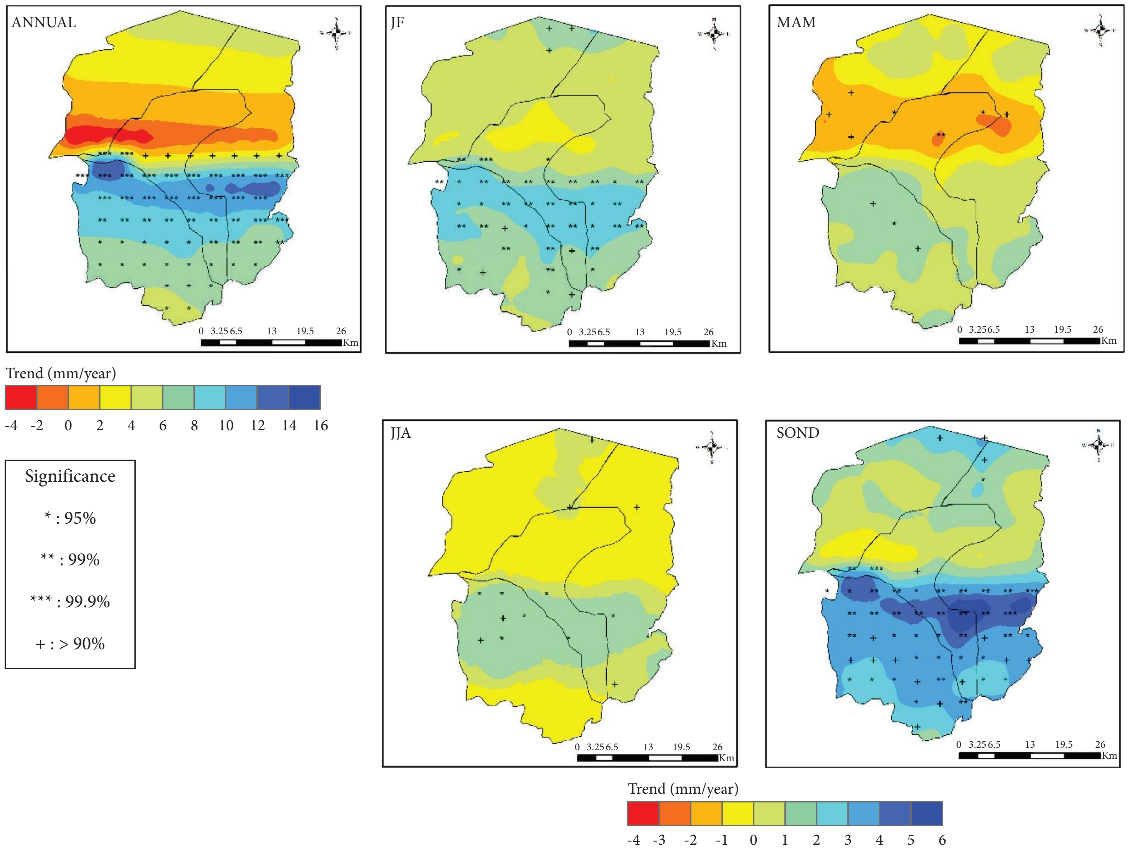

Figure 8: Spatial rainfall trend during January to February (JF), March to May (MAM), June to August (JJA), September to December (SOND), and annual time scale over the Kayonza District from 1981 to 2021. The significance of the trend is given as above 90% (+), 95% (*), 99% (**), and 99.9% (***) significance level, respectively. JF, MAM, JJA, and SOND share the same legend.

Graphical trend analysis for different climatic zones for different seasons and the annual time scale were analyzed for the period of 1981 to 2021. The trend results for the short dry season (JF) are presented in Figure 9, and those for the long dry season (JJA) are indicated in Figure 10. When averaged over the climatological zone, the region one (R1) shows a decreasing trend for both dry seasons, while a small increase was observed over the region two (R2). However, both region three (R3) and region four (R4) show an increase in seasonal rainfall for both short and long dry seasons. These results suggest a general increase during dry seasons which would have an impact on the postharvest for the two growing seasons and would suggest an implementation of the measures that enhance the handling of yield and used for preparation of the subsequent growing period. Figure 11 indicates the obtained trend results for wet seasons of MAM season, while Figure 12 shows the trend results for the SOND season. It is clearly seen that areas located in region one (R1) show a decreasing trend for both wet seasons, while those in region two (R2) show a reduced magnitude during the MAM season, while an upward slop was observed during the SOND season. Similarly, a decrease in region three (R3) during the MAM season and positive slope during the SOND season, while a negative trend during MAM and a positive trend during SOND were indicated over region (R4). For the annual time scale (Figure 13), except for region one (R1) which indicated a reduced trend, an increased rainfall was observed in the rest of the regions with higher increase over regions three and four (R3 and R4).

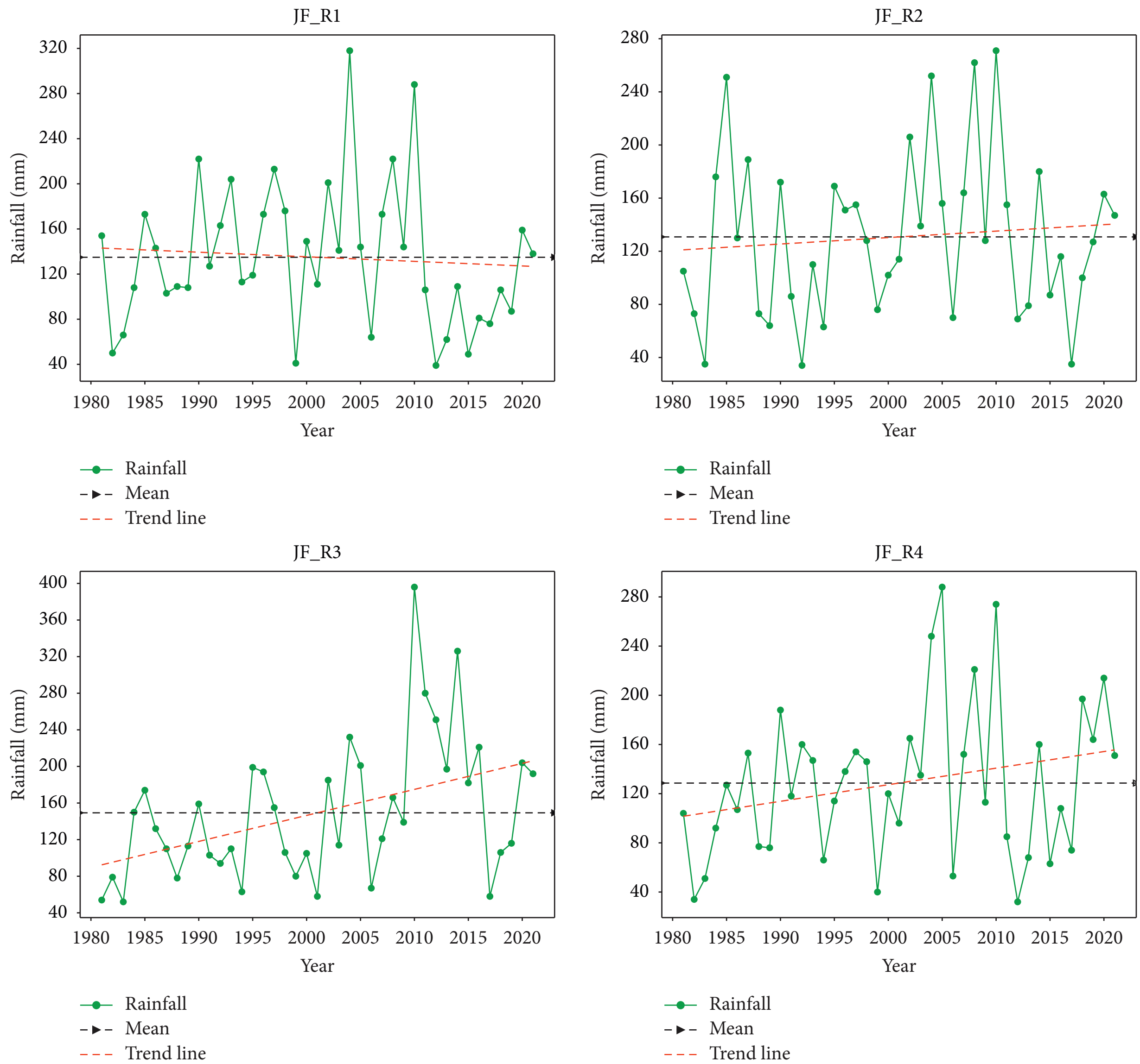

Figure 9: Rainfall trend during January to February (JF) seasonal time scale for region one (R1), region two (R2), region three (R3), and region four (R4) over the Kayonza District from 1981 to 2021.

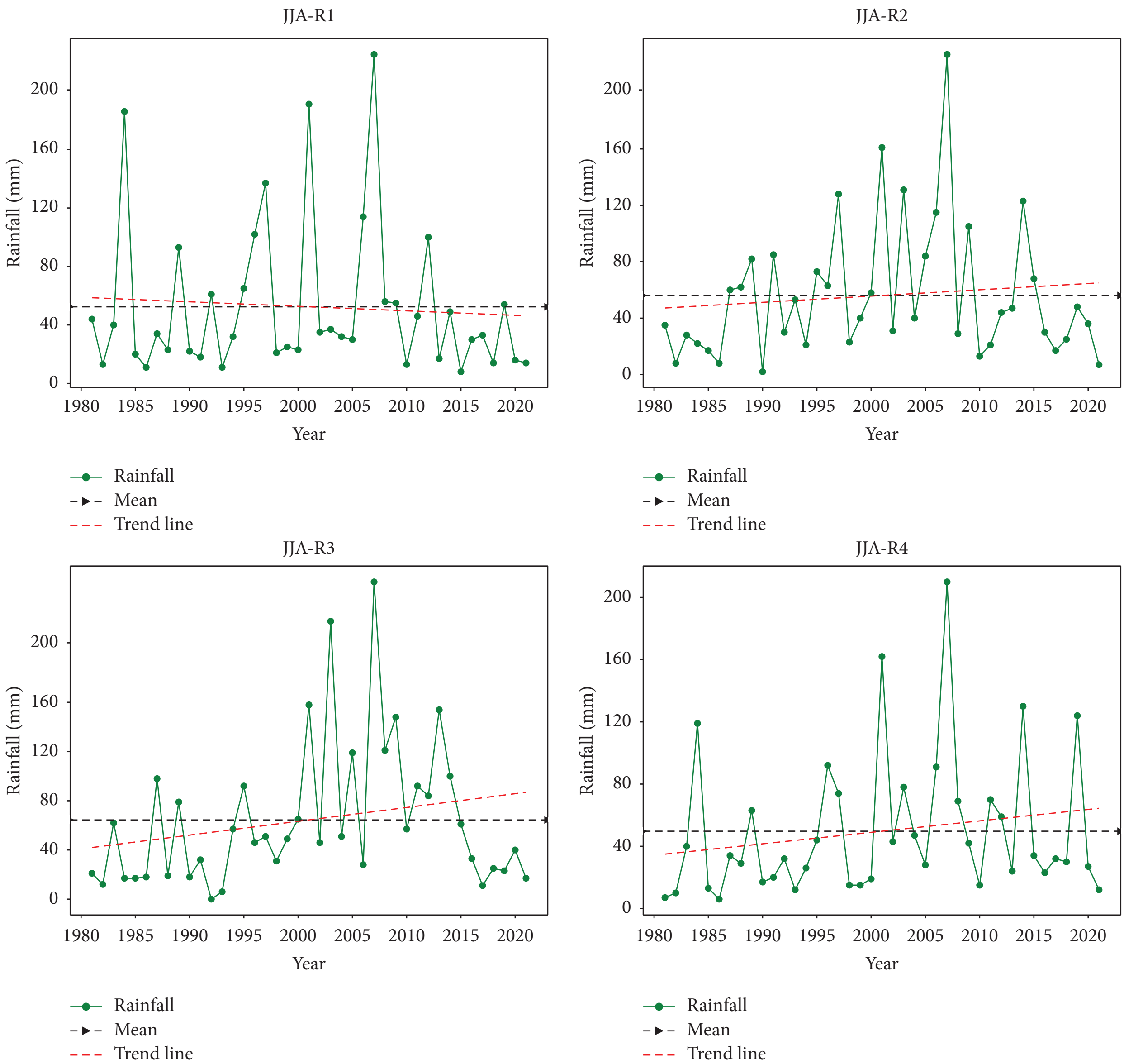

FIGURE 10: Rainfall trend during June to August (JJA) seasonal time scale for region one (R1), region two (R2), region three (R3), and region four (R4) over the Kayonza District from 1981 to 2021.

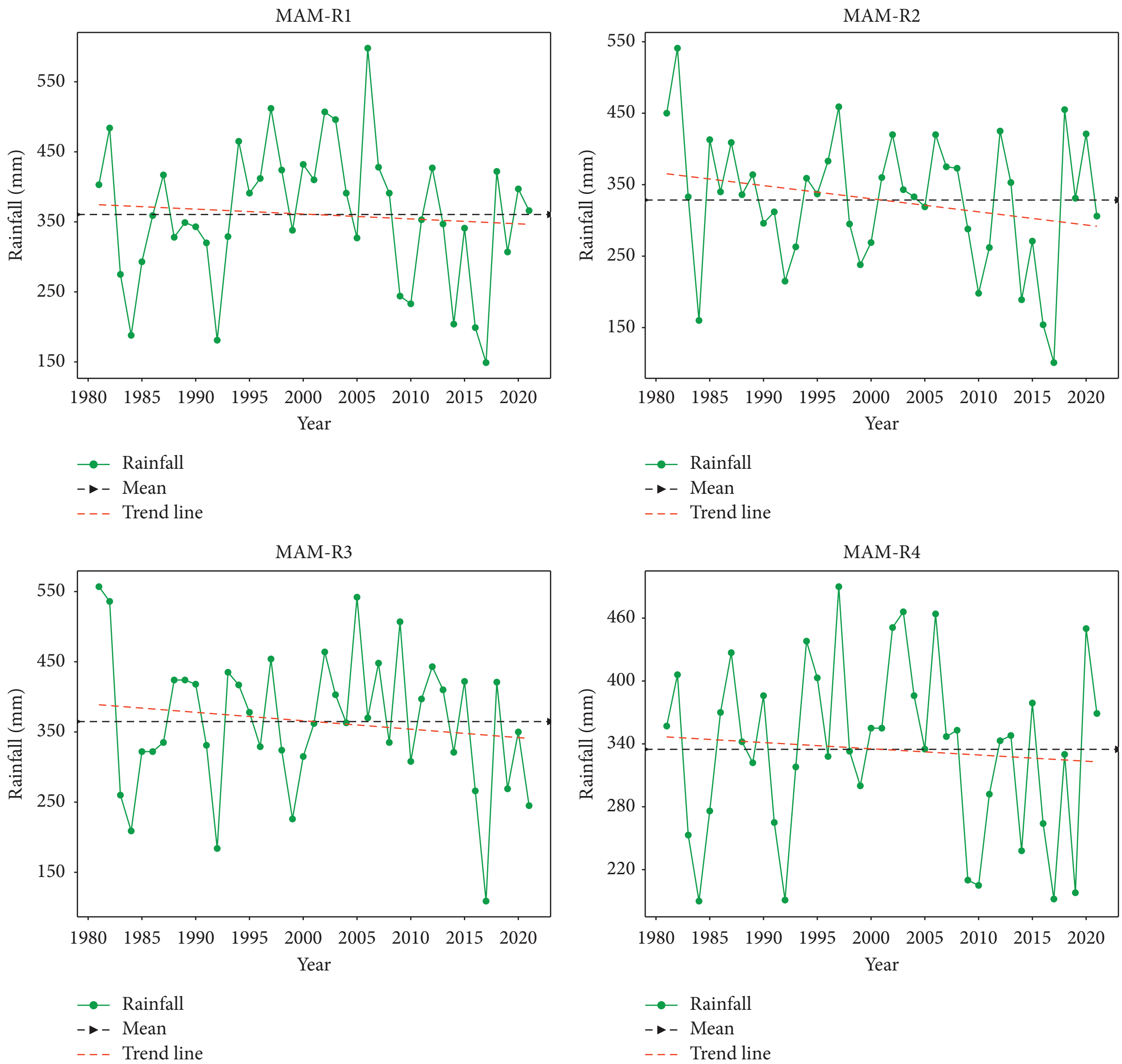

Figure 11: Rainfall trend during March to May (MAM) seasonal time scale for region one (R1), region two (R2), region three (R3), and region four (R4) over the Kayonza District from 1981 to 2021.

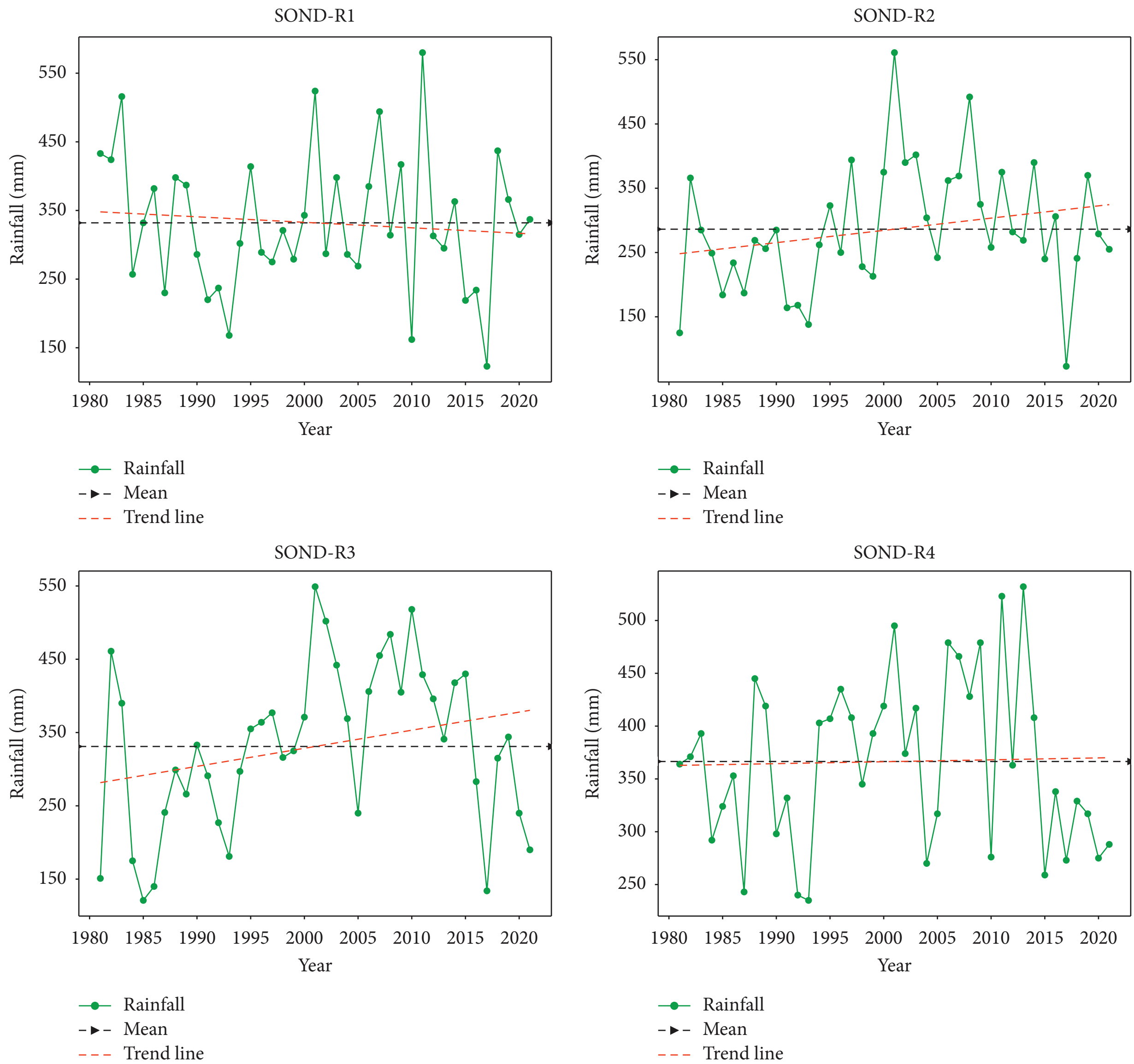

Figure 12: Rainfall trend during September to December (SOND) seasonal time scale for region one (R1), region two (R2), region three (R3), and region four (R4) over the Kayonza District from 1981 to 2021.

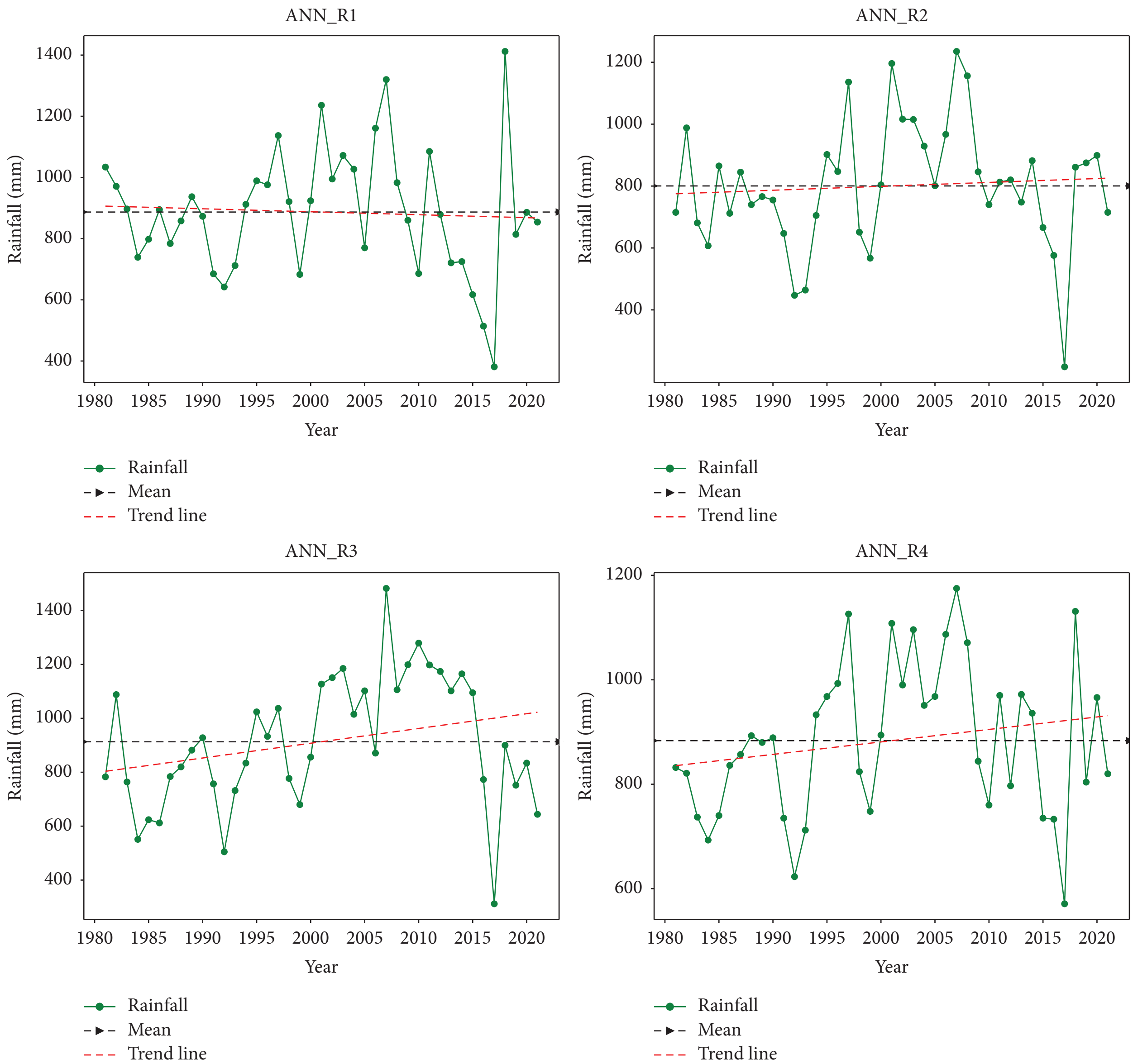

FIGURE 13: Annual rainfall trend for region one (R1), region two (R2), region three (R3), and region four (R4) over the Kayonza District from 1981 to 2021.

4. Conclusions

In this paper, we aim to explore the variability and trends in rainfall using the coefficient of variation and a nonparametric approach. Through the *K*-means clustering technique, four near homogeneous climate zones were found. In the past four decades, there have been significant variations in both dry seasons. The data summary makes it clear that the district is getting considerably less rain, which is also distributed unevenly around the area. In addition, it is exhibiting a declining trend, albeit a nonsignificant one, especially in the northern part, while a significant upward trend was seen in the central part throughout the brief dry and rainy seasons as well as on an annual time scale. Increased precipitation during SOND and JF would be beneficial to agricultural activities, though the postharvest period would be impacted, raising serious concerns among environmentalists, climatologists, farmers, policymakers, and the general public. In light of this, the results of this study are crucial for an agrarian economy like ours. The findings of this study are essential for creating adequate mitigation strategies to lessen climate change's effects on agriculture as well as other socioeconomic sectors in the district and also highlights the need for further analysis of the extreme events and intraseasonal characteristics as well as future projection studies for planning and decision-making purposes aiming at the development of the areas.

Data Availability

The rainfall and temperature dataset used in the present study was obtained from the Rwanda Meteorology Agency (Meteo Rwanda). The dataset is available by request through online services at https://www.meteorwanda.gov.rw.

Conflicts of Interest

The authors declare that they have no conflicts of interest.

Acknowledgments

The authors are grateful to the Rwanda Meteorology Agency for providing relevant data for this article.

References

[1] A. Ayanlade, A. Oluwaranti, O. S. Ayanlade et al., "Extreme climate events in sub-Saharan Africa: a call for improving agricultural technology transfer to enhance adaptive capacity," *Climate Services*, vol. 27, Article ID 100311, 2022.

[2] T. Mabhaudhi, S. Mpandeli, L. Nhamo et al., "Prospects for improving irrigated agriculture in Southern Africa: linking water, energy and food," *Water (Switzerland)*, vol. 10, no. 12, pp. 1881–1916, 2018.

[3] V. Bjornlund, H. Bjornlund, and A. F. Van Rooyen, "Why agricultural production in sub-Saharan Africa remains low compared to the rest of the world–a historical perspective," *International Journal of Water Resources Development*, vol. 36, no. 1, pp. S20–S53, 2020.

[4] T. Jayne, L. Fox, K. Fuglie et al., "Agricultural productivity growth, resilience, and economic transformation in sub-saharan Africa implications for USAID," *Association of Public and Land-Grant Universities*, vol. 104, 2021.

[5] O. Peter, O. Laban, O. Raphael, H. Herry, and W. Mathewe, "East african rainfall variability associated with the madden-julian oscillation," *Journal of Kenya Meteorological Society*, vol. 2, pp. 105–114, 2008.

[6] C. Funk, M. D. Dettinger, J. C. Michaelsen et al., "Warming of the Indian Ocean threatens eastern and southern African food security but could be mitigated by agricultural development," *Proceedings of the National Academy of Sciences*, vol. 105, no. 32, pp. 11081–11086, 2008.

[7] S. E. Nicholson, "Climate and climatic variability of rainfall over eastern Africa," *Reviews of Geophysics*, vol. 55, no. 3, pp. 590–635, 2017.

[8] X. Zhou, L. Chen, J. Umuhoza, Y. Cheng, L. Wang, and R. Wang, "Intraseasonal oscillation of the rainfall variability over Rwanda and evaluation of its subseasonal forecasting skill," *Atmospheric and Oceanic Science Letters*, vol. 14, no. 6, Article ID 100099, 2021.

[9] A. Nkunzimana, B. Shuoben, W. Guojie et al., "Assessment of drought event, its trend and teleconnected factors over Burundi, Central East Africa," *Theoretical and Applied Climatology*, vol. 145, no. 3-4, pp. 1293–1316, 2021.

[10] P. G. Oguntunde, B. J. Abiodun, G. Lischeid, and C. Merz, "Modelling the impacts of reforestation on the projected hydroclimatology of Niger river basin, west Africa," *Ecohydrology*, vol. 7, no. 1, pp. 163–176, 2014.

[11] C. Wenhaji Ndomeni, E. Cattani, A. Merino, and V. Levizzani, "An observational study of the variability of East African rainfall with respect to sea surface temperature and soil moisture," *Quarterly Journal of the Royal Meteorological Society*, vol. 144, no. 1, pp. 384–404, 2018.

[12] C. C. Mutai and M. N. Ward, "East african rainfall and the tropical circulation/convection on intraseasonal to interannual timescales," *Journal of Climate*, vol. 13, no. 22, pp. 3915–3939, 2000.

[13] W. Nyakwada, L. A. Ogallo, and R. E. Okoola, "The atlantic-Indian Ocean Dipole and its influence on east african seasonal rainfall," *Journal of Meteorology and Related Sciences*, vol. 3, pp. 21–35, 2009.

[14] Z. Owiti, "Linkages between the Indian Ocean Dipole and east african seasonal rainfall anomalies national council for science and technology IGAD climate prediction and Applications centre," *Journal of Kenya Meteorological Society Volume*, vol. 2, pp. 3–17, 2008.

[15] R. E. Okoola, "A diagnostic study of the eastern Africa monsoon circulation during the northern hemisphere spring season," *International Journal of Climatology*, vol. 19, no. 2, pp. 143–168, 1999.

[16] M. Indeje, F. H. M. Semazzi, and L. J. Ogallo, "ENSO signals in East African rainfall seasons," *International Journal of Climatology*, vol. 20, no. 1, pp. 19–46, 2000.

[17] B. Liebmann, M. P. Hoerling, C. Funk et al., "Understanding recent eastern Horn of Africa rainfall variability and change," *Journal of Climate*, vol. 27, no. 23, pp. 8630–8645, 2014.

[18] I. Muhire, F. Ahmed, and K. Abutaleb, "Relationships between Rwandan seasonal rainfall anomalies and ENSO events," *Theoretical and Applied Climatology*, vol. 122, no. 1–2, pp. 271–284, 2015.

[19] K. Jonah, W. Wen, S. Shahid et al., "Spatiotemporal variability of rainfall trends and influencing factors in Rwanda," *Journal of Atmospheric and Solar-Terrestrial Physics*, vol. 219, Article ID 105631, 2021.

[20] R. B. Stothers, "Volcanic eruptions and climate change," *Encyclopedia of Earth Sciences Series*, vol. 38, no. 2, pp. 976–979, 2000.

[21] G. Chen, "A model of the convectively coupled equatorial Rossby wave over the indo-pacific warm pool," *Journal of the Atmospheric Sciences*, vol. 79, no. 9, pp. 2267–2283, 2022.

[22] P. Omeny, L. Ogallo, R. Okoola, H. Hendon, and M. Wheeler, "East African rainfall variability associated with the Madden-Julian oscillation," *Journal of Kenya Meteorological Society*, vol. 2, no. 2, pp. 105–114, 2008.

[23] L. Ilunga, I. Muhire, and C. Mbaragijimana, "Saisons pluviométriques et origine des pluies au Rwanda," *Geo-Eco-Trop*, vol. 28, no. 1–2, pp. 61–68, 2004.

[24] M. Kizza, A. Rodhe, C. Xu, H. K. Ntale, and S. Halldin, "Temporal rainfall variability in the lake Victoria basin in East Africa during the twentieth century," *Theoretical and Applied Climatology*, vol. 98, no. 1-2, pp. 119–135, 2009.

[25] L. Ilunga and I. Muhire, "Comparaison des fluctuations des précipitations moyennes annuelles au Rwanda avec les épisodes EL NIÑO/LA NIÑA et les cycles des taches solaires," *Geo-Eco-Trop*, vol. 34, no. 34, pp. 75–86, 2010.

[26] C. C. Mutai and M. N. Ward, "East African rainfall and the tropical circulation/convection on intraseasonal to interannual timescales," *Journal of Climate*, vol. 13, no. 22, pp. 3915–3939, 2000.

[27] A. Siebert, T. Dinku, F. Vuguziga, A. Twahirwa, and D. M. Kagabo, "Evaluation of ENACTS-Rwanda:a new multi-decade, high-resolution rainfall and temperature data set—climatology," *International Journal of Climatology*, vol. 39, no. 6, pp. 3104–3120, 2019.

[28] M. A. Umutoni, L. P. Japheth, E. J. Lipiki, L. L. Kebacho, P. T. S. Limbu, and E. K. Makula, "Investigation of the 2016 March to may extreme rainfall over Rwanda," *Natural Hazards*, vol. 108, no. 1, pp. 607–618, 2021.

[29] N. J. Sebaziga, F. Ntirenganya, A. Tuyisenge, and V. Iyakaremye, "A statistical analysis of the historical rainfall data over eastern Province in Rwanda," *East African Journal of Science and Technology*, vol. 10, no. 1, pp. 33–52, 2020.

[30] I. Muhire, F. Ahmed, and M. A. M. A. Elbasit, "Spatio-temporal variations of rainfall erosivity in Rwanda," *Journal of Soil Science and Environmental Management*, vol. 6, no. 4, pp. 72–83, 2015.

[31] D. Ntwali, B. A. Ogwang, and V. Ongoma, "The impacts of topography on spatial and temporal rainfall distribution over Rwanda based on WRF model," *Atmospheric and Climate Sciences*, vol. 06, no. 02, pp. 145–157, 2016.

[32] H. S. Endris, C. Lennard, B. Hewitson, A. Dosio, G. Nikulin, and G. A. Artan, "Future changes in rainfall associated with ENSO, IOD and changes in the mean state over Eastern Africa," *Climate Dynamics*, vol. 52, no. 3–4, pp. 2029–2053, 2019.

[33] J. Umuhoza, L. Chen, and L. Mumo, "Assessing the skills of Rossby centre regional climate model in simulating observed rainfall over Rwanda," *Atmospheric and Climate Sciences*, vol. 11, no. 03, pp. 398–418, 2021.

[34] J. Uwimbabazi, Y. Jing, V. Iyakaremye, I. Ullah, and B. Ayugi, "Observed changes in meteorological drought events during 1981–2020 over Rwanda, East Africa," *Sustainability*, vol. 14, no. 3, p. 1519, 2022.

[35] B. Mushonga, L. Hategekimana, G. Habarugira, E. Kandiwa, A. Samkange, and B. V. Ernest Segwagwe, "Characterization of the beekeeping value chain: challenges, perceptions, limitations, and opportunities for beekeepers in Kayonza district, Rwanda," *Advances in Agriculture*, vol. 2019, Article ID 5982931, 9 pages, 2019.

[36] National Insititute of statistics of Rwanda, "Fourth population and housing census, Rwanda," *Thematic Report Population Size, Structure and Distribution*, 2014.

[37] F. Ndayisaba, H. Guo, A. Bao, H. Guo, F. Karamage, and A. Kayiranga, "Understanding the spatial temporal vegetation dynamics in Rwanda," *Remote Sensing*, vol. 8, no. 2, pp. 129–217, 2016.

[38] H. Mohammed, C. K. Jean, and W. A. Ahmad, "Projections of precipitation, air temperature and potential evapotranspiration in Rwanda under changing climate conditions," *African Journal of Environmental Science and Technology*, vol. 10, no. 1, pp. 18–33, 2016.

[39] S. Niyonasenze, P. Mulyungi, and E. N. Shukla, "AN effective policy strategy for utilization of fragmented lands in Rwanda: land use consolidation from farmers perspectives," *International Journal of Agricultural Extension and Rural Development Studies*, vol. 5, no. 4, pp. 38–42, 2017.

[40] I. Muhire and F. Ahmed, "Spatio-temporal trend analysis of precipitation data over Rwanda," *South African Geographical Journal*, vol. 97, no. 1, pp. 50–68, 2015.

[41] I. Muhire and F. Ahmed, "Spatiotemporal trends in mean temperatures and aridity index over Rwanda," *Theoretical and Applied Climatology*, vol. 123, no. 1–2, pp. 399–414, 2016.

[42] S. M. Henninger, "Does the global warming modify the local Rwandan climate?" *Natural Science*, vol. 05, no. 01, pp. 124–129, 2013.

[43] I. Muhire and F. Ahmed, "Spatio-temporal trends in major food crop yields in Rwanda," *Global Journals Inc., USA*, vol. 14, pp. 25–42, 2014.

[44] I. Muhire and F. Ahmed, "Yields of major food crops responses to changing and varying climate in Rwanda," *Agricultural Science Research Journal*, vol. 4, no. 11, pp. 181–192, 2014.

[45] J. P. Ngarukiyimana, Y. Fu, C. Sindikubwabo et al., "Climate change in Rwanda: the observed changes in daily maximum and minimum surface air temperatures during 1961–2014," *Frontiers in Earth Science*, vol. 9, 2021.

[46] B. Safari, J. N. Sebaziga, and A. Siebert, "Evaluation of CORDEX-CORE regional climate models in simulating rainfall variability in Rwanda," *International Journal of Climatology*, vol. 43, no. 2, pp. 1112–1140, 2023.

[47] A. Twahirwa, C. Oludhe, P. Omondi, G. Rwanyiziri, S. Ndakize, and S. Guhirwa, "Analysis of climate change indices in musanze district, Rwanda," *Journal of Climate Change and Sustainability*, vol. 4, no. 1, pp. 17–25, 2022.

[48] N. J. Sebaziga, B. Safari, N. J. Ngaina et al., "Rainfall variability and trends over Rwanda," *Journal of Climate Change and Sustainability*, vol. 4, no. 1, pp. 26–34, 2022.

[49] M. A. W. Atanabe, "Application of cluster analysis to climate model performance metrics," *Journal of Applied Meteorology and Climatology*, vol. 50, pp. 1666–1675, 2011.

[50] S. Singh and N. S. Gill, "Analysis and study of K-means clustering algorithm," *Int. J. Eng. Res. Technol.*, vol. 2, no. 7, pp. 2546–2551, 2013.

[51] R. Pitri, A. M. Soleh, and A. Djuraidah, "Statistical downscaling modeling through k-means clustering," *International Journal of Scientific*, vol. 4, no. 9, pp. 220–227, 2018.

[52] S. Sriadhi, S. Gultom, and M. Martiano, "Accuracy of data cluster using modify K-mean algorithm by local deviation method faculty of engineering," *Universitas Negeri Medan, Indonesia*, vol. 29, no. 5, pp. 2019–2025, 2020.

[53] C. Series, "K-means clustering algorithm and its improvement," *Journal of Physics: Conference Series*, vol. 1873, 2021.

[54] A. Wickramasinghe, S. Muthukumarana, D. Loewen, and M. Schaubroeck, "Temperature clusters in commercial buildings using k-means and time series clustering," *Energy Informatics*, vol. 5, no. 1, pp. 1–14, 2022.

[55] E. Biabiany, D. C. Bernard, and V. Page, "Design of an expert distance metric for climate clustering:the case of rainfall in the Lesser Antilles," *Computers and Geosciences*, vol. 145, Article ID 104612, 2020.

[56] Y. Wan, Q. Xiong, Z. Qiu, and Y. Xie, "SS symmetry K-means clustering algorithm based on memristive chaotic system and sparrow search algorithm," *Symmetry*, vol. 14, 2022.

[57] V. Ongoma, H. Chen, and C. Gao, "Projected changes in mean rainfall and temperature over East Africa based on CMIP5 models," *International Journal of Climatology*, vol. 38, no. 3, pp. 1375–1392, 2017.

[58] F. Wang, W. Shao, H. Yu et al., "Re-Evaluation of the power of the mann-kendall test for detecting monotonic trends in hydrometeorological time series," *Frontiers in Earth Science*, vol. 8, pp. 1–12, 2020.

[59] S. A. Diress and T. B. Bedada, "Precipitation and temperature trend analysis by Mann kendall test: the case of addis ababa methodological station, addis ababa, Ethiopia," *African Journal on Land Policy and Geospatial Sciences*, vol. 4, no. 4, p. 518, 2021.

[60] A. Sanogo, R. S. Kabange, P. A. Owusu, B. I. Djire, R. F. Donkoh, and N. Dia, "Investigation into recent temperature and rainfall trends in mali using mann-kendall trend test:case study of bamako," *Journal of Geoscience and Environment Protection*, vol. 11, pp. 155–172, 2023.

[61] B. Safari, "Trend analysis of the mean annual temperature in Rwanda during the last fifty two years," *Journal of Environmental Protection*, vol. 03, no. 06, pp. 538–551, 2012.
[62] L. Ding and H. W. Kinnucan, "This document is discoverable and free to researchers across the globe due to the work of AgEcon Search. Help ensure our sustainability," *Journal of Gender, Agriculture and Food Security*, vol. 1, no. 3, pp. 1–22, 2011.
[63] T. E. Stathers, R. Lamboll, and B. M. Mvumi, "Post-harvest agriculture in a changing climate," *International Journal of Rural Development*, vol. 47, no. 1, pp. 1–3, 2013.
[64] H. Hengsdijk and W. J. de Boer, "Post-harvest management and post-harvest losses of cereals in Ethiopia," *Food Security*, vol. 9, no. 5, pp. 945–958, 2017.
[65] D. Kumar and P. Kalita, "Reducing postharvest losses during storage of grain crops to strengthen food security in developing countries," *Foods*, vol. 6, no. 1, pp. 8–22, 2017.
[66] S. W. Ndiritu and R. D. Ruhinduka, "Climate variability and post-harvest food loss abatement technologies: evidence from rural Tanzania," *Studies in Agricultural Economics*, vol. 121, no. 1, pp. 30–40, 2019.